Research Article

Adipose-Derived Mesenchymal Stem Cells Extracellular Vesicles (ADMSCs-EVs) Implantation in Critical Size Bone Defect Model: Callus Formation Histology, BMP2, and Wnt Signaling

Iqra Kousar,[1,2] Ismail H. Dilogo, [2,3,4] Radiana D. Antarianto,[2,5*] Jeanne A. Pawitan,[2,4,5] Amer Mahmood,[6] Rahyussalim[2,3,4]

[1]Master Program in Biomedical Science Faculty of Medicine Universitas Indonesia, Jakarta, Indonesia
[2]Stem Cell and Tissue Engineering Research Cluster IMERI Faculty of Medicine Universitas Indonesia, Jakarta, Indonesia
[3]Department of Orthopaedics and Traumatology, Faculty of Medicine Universitas Indonesia, Cipto Mangunkusumo Hospital, Jakarta, Indonesia
[4]Integrated Service Unit Stem Cells Technology Cipto Mangunkusumo Hospital, Jakarta, Indonesia
[5]Department of Histology Faculty of Medicine Universitas Indonesia, Jakarta, Indonesia
[6]Stem Cell Unit Department of Anatomy, King Saud University, Riyadh, Kingdom Saudi Arabia

Abstract

Critical bone defects pose a substantial healthcare burden globally. This study aimed to investigate the miRNA content adipose-derived mesenchymal stem cells extracellular vesicles (ADMSCs-Evs) or exosomes, which affected critical-sized bone histology, BMP2, and Wnt signalling pathways. Total RNA extraction and microarray analysis of miRNA were conducted. In-vivo experiments were performed on 16 critical-sized bone defect SD rats (eight for ADMSCs-EVs/exosomes and eight for NaCl) and four healthy control SD rats. The rats from each group were sacrificed on day 14 and day 28. Bone defect samples were collected for histology, protein, and molecular analysis. Histology analysis revealed increasing soft callus formation in the ADMSCs-Evs (exosomes) treated group on days 14 and 28 compared to the negative control group. Downregulation of miR-433-3p, miR-542-3p, and miR-328-3p in ADMSCs-Evs (exosomes) enhances Wnt3A expression. Upregulation of miR-93-5p in ADMSCs-Evs (exosomes) inhibits BMP2 signalling, confirmed by BMP2 ELISA and higher chordin (BMP-2 antagonist) expression. Spp1 as a downstream gene of BMP-2 and Wnt signalling are indifferent. Specific miRNA inside ADMSCs-EVs (exosomes) regulates BMP-2 and Wnt signalling to enhance soft callus formation in critical size bone defect in EVs treated group than in negative control.

Keywords: exosomes, miRNA, BMP2, Wnt, critical sized bone defect.

Implantasi Vesikel Ekstraseluler Asal Sel Punca Mesenkimal Adiposa (ADMSs-EVs) pada Model Defek Tulang Kritis: Histologi Pembentukan Kalus, BMP2, dan Persinyalan Wnt

Abstrak

Defek tulang kritis menimbulkan beban kesehatan yang signifikan di seluruh dunia. Penelitian ini bertujuan untuk mengkarakterisasi isi miRNA ADMSCs-EVs (eksosom) dan efek ADMSCs-EVs (eksosom) pada histologi defek tulang kritis, ekspresi BMP2, dan Wnt. Dilakukan ekstraksi total RNA dan analisis microarray miRNA. Eksperimen in-vivo pada 16 model tikus SD defek tulang kritis delapan untuk ADMSCs-EVs/eksosom dan delapan untuk NaCl) ditambah empat tikus SD kontrol yang sehat. Tikus dari masing-masing kelompok dikorbankan pada hari ke-14 dan ke-28. Sampel defek tulang kritis dianalisis secara histologi, protein, dan molekuler. Satu potongan memanjang dari sampel tulang diproses untuk analisis histologis seperti pewarnaan HE dan Masson trikrom. Analisis histologi menunjukkan peningkatan terbentuknya kalus lunak di defek tulang kritis pada hari ke-28 dibandingkan hari ke-14. Penurunan ekspresi miR-433-3p, miR-542-3p, dan miR-328-3p pada ADMSCs-EVs (eksosom) meningkatkan pensinyalan Wnt sementara peningkatan ekspresi miR-93-5p pada ADMSCs-EVs (eksosom) menghambat sinyal BMP2 yang dikonfirmasi oleh ELISA BMP2 dan peningkatan ekspresi chordin (antagonis BMP2). Ekspresi gen Spp1 sebagai target gen jalur BMP2 dan Wnt tidak mengalami perubahan. miRNA spesifik dalam ADMSCs-Evs (eksosom) mengatur jalur sinyal BMP2 dan Wnt sehingga meningkatkan pembentukan kalus lunak di defek tulang kritis.

Kata kunci: eksosom, miRNA, BMP-2, Wnt, defek tulang kritis.

Introduction

Critical bone defects, classified by the loss of more than 50% diameter or defects exceeding 2 cm in length in long bones[1], present a substantial healthcare burden, with around 100,000 reported cases annually in the USA, incurring costs of approximately $2.5 billion.[2-4] In Indonesia, from 1997 to 2001, there was a 4-fold increase in the need for bone grafts with an increase in cases of bone damage.[5] Moreover, Dilogo et al[6] reported that in dr. Cipto Mangunkusumo, RSCM Kencana, Indonesia, bone defect-related reconstruction procedures are required in 27% of all fracture cases.[6] Such bone defects carry risks of complications, including nonunion, malunion, and deep infection. To face this challenge, many research investigations have been done to heal bone defects. In a study by Dilogo et al[7], white male Sprague Dawley rats were used as the animal model, where a 5 mm critical bone defect was induced in the femur bone and stabilized utilizing a 1.4 mm threaded intramedullary Kirschner wire fixation method.[7]

Treatment of extensive bone defects remains challenging despite advancements in treatment modalities.[1,8] Current treatment approaches involve autologous bone grafts, proper fixation, and the in-situ application of various materials.[4,9,10] However, autologous grafts have limitations such as donor morbidity, limited availability, and unreliable rates of osteogenesis. Defects larger than 5 cm typically require more than autologous grafts for effective treatment. The treatment of extensive bone defects is increasingly developing with stem cells.[11] Mesenchymal stem cells (MSCs) have a multipotent nature, high renewing ability and rapid proliferation and can be easily obtained from various sources, such as blood, adipose tissue, umbilical cord, dental components, and bone marrow. MSCs from adipose tissue (ADMSCs) are more accessible to isolate using simple washing coffee filter methods[12], and their cell proliferation is faster and more abundant than that of MSCs from other sources.[7] Osteogenic differentiated adipose MSCs have been demonstrated to have excellent bone healing capacity.[13] ADMSCs have several drawbacks, such as cell senescence and invasive procedures to obtain lipoaspirate, which certified plastic surgeons and dermatovenereologists must perform. The therapeutic effect of MSCs in bone regeneration can be elaborated by direct differentiation into osteocytes and secretion of paracrine factors. One of the paracrine factors released by MSCs is extracellular vesicles (EVs).[14]

EVs are membranous lipid bilayer structures ranging in size from 30 to 1000 nm. EVs produced by mesenchymal stem cells influence bone regeneration signalling pathways such as Wnt and BMP-2.[15] ADMSCs-EVs can potentially regulate the healing process of bone defects both positively and negatively. There is a significant research gap regarding the study of ADMSCs-EVs and their potential to regenerate critical-sized bone defects. This study aimed to investigate the characteristics of ADMSCs-EVs, specifically miRNA content, and the effect of EVs AD MSCs on critical-sized bone defect histology, BMP2, and Wnt expressions.

Methods

This study was performed at the Stem Cell and Tissue Engineering (SCTE), Animal Research Facility (ARF), and Molecular Biology and Proteomic Core Facilities (MBPCF) of Indonesia Medical Education and Research Institute (IMERI), Department of Histology Laboratory Faculty of Medicine Universitas Indonesia (FMUI), Integrated Laboratory & Research Center (ILRC) Universitas Indonesia Laboratory, the Forensic Laboratory Center for the Criminal Investigation Agency Indonesian National Police (Puslabfor Bareskrim Polri), and the Nanostring Genetica Science laboratory. All procedures conducted in this study have been approved by The Ethical Committee FMUI No. 414/UN2.F1/ETIK/2023, valid until 31.03.2024.

The samples for this study were (i) ADMSCs-EVs that were isolated from a conditioned medium (CM) of ADMSC culture, (ii) critical-sized femoral bone defects samples from 16 Sprague Dawley (SD) rats, (iii) healthy femoral bone samples from 4 SD rats. The inclusion criteria for the rats are 2-month-old male rats weighing 150-260 grams without clinical physical disabilities. The exclusion criteria are rats with lower extremities dysfunctions before surgery and rats who died before days 14 and 28 after surgery.

ADMSC Culture

Human ADMSCs cryovials were retrieved from the SCTE IMERI liquid nitrogen tank (Statebourne/ Biorack 750, UK), thawed, and seeded according to the following protocol. The ADMSC culture medium was prepared with 87% (v/v) αMEM (Gibco, USA -12571063), 10% PRP (Indonesian Red Cross Blood Type O, Rhesus +, Indonesia), 1% heparin (1000U/ mL) (Inviclot heparin sodium 5000 IU/mL, Indonesia), 1% Antibiotic and Antimycotic (ABAM) (Gibco, USA -15240062), and 1% Glutamax (Gibco, USA -35050061). Nine millilitres of ADMSC culture medium were mixed with one millilitre of thawed ADMSCs and centrifuged at 1200 rpm for 10 minutes. After centrifugation, the cell pellets were resuspended in the

ADMSC culture medium. The resuspended cells were then counted using the trypan blue exclusion method with trypan blue reagent (Gibco, USA -15250061) in a Neubauer-improved counting chamber (Indonesia). ADMSCs were seeded into a 75 cm² flask at 5 × 10³ cells per cm² density and cultured in a 5% CO2 incubator (D180 180-260VAC, China) at 37°C. The culture medium was replaced every 2-3 days, and the old medium was collected from five passages.

Exosomes Isolation

To obtain the conditioned medium (CM), the MSCs that reached 70% confluency were removed from the culture medium. The culture medium was replaced every 2-3 days. Before medium replacement, the culture flask was washed with 0.1 µm filtered PBS [(Gibco, USA)™ -10010023] for one wash. Next, the CM was collected and replaced with a complete MSC medium. The collected medium was stored at -20°C until ready to use. EVs were isolated from the collected CM using an ultracentrifugation technique following the copyright protocol established in SCTE IMERI.[16] The conditioned medium was centrifuged at 750 × g for 15 min at 20°C to discard cells, at 2000 × g for 15 min, and at 10,000 × g for 45 min to remove cell debris and large vesicles, respectively. The resulting supernatant was filtered with a 0.2 µm syringe filter (S6534-TMOSK-sartorius, Germany).

Exosomes were then isolated by ultracentrifugation at 100,000 × g and 4°C for 90 minutes using an ultracentrifugation machine [(Thermo-Scientific, USA) -75000100]. The supernatant was discarded, and the exosome pellet was transferred from the ultracentrifugation tube to a 15 ml Falcon tube. The exosomes were dissolved in cold D-PBS [(Gibco, USA)™ -14190144] until the volume reached 5 mL then re-suspension was performed. Exosomes were then aliquoted into a 1 mL cryovial and stored in a cryo-box chiller with a temperature of -20°C or freezer with a temperature of -80°C for 1-year storage. Freshly purified EVs were used for animal experiments. Sterility testing, particle size analysis (PSA), and zeta potential measurements confirmed that the pallet contained exosomes and met the MISEV 2018 guidelines.

RNA Extraction

There were two different kinds of samples: ADMSCs-Evs (exosomes) and critical bone defect samples. Both types of samples had different pre-RNA extraction preparations, but both types of samples followed the same RNA extraction protocol. Preparation of solid bone defect samples, which

were already placed in 1000 µl of DNA/RNA Shield™ (1X), underwent sequential homogenization steps, initially manually with a mortar, followed by further homogenization utilizing a homogenizer (DATHAN Scientific). RNA was isolated from ADMSCs-EVs (exosomes) and homogenized bone defect samples using an RNA Isolation Quick RNA Miniprep Plus Kit (R1058-Zymo Research, USA). 30µl of PK Digestion Buffer and 15µl of Proteinase K were mixed into the 300µl homogenized samples. After a thorough mix, the samples were incubated for 30 minutes at 55°C. The incubated samples were then vortexed and centrifuged (microcentrifuge [Thermo Scientific]) for 2 minutes at maximum speed. The supernatant of each sample was then transferred into a 1.5 mL tube, where it was mixed with the same amount of RNA Lysis Buffer.

Purification of the samples was done by transferring samples into a Spin-Away™ Filter (yellow) in a collection tube and centrifuging for 30 seconds at 16,000xg at room temperature. The solution that was passed to the collection tube (flow-through) was taken and then added with absolute ethanol in a ratio of 1:1. After mixing, the samples were transferred into a Zymo-Spin™ IIICG Column (green) in a collection tube and finally centrifuged under the same conditions as before. The column was then splashed with 400µl of RNA wash buffer and centrifuged, and the flow-through was discarded. Using a separate 75µl DNA digestion buffer and 5µl DNase I, the mixture was made in a 1.5 mL tube. This mixture was added to the previous column matrix before being incubated for 15 minutes at room temperature and 400µl of RNA prep buffer was mixed into a column and again centrifuged under the same conditions, and the flow-through was discarded. 700µl of RNA wash buffer mixed into the column and repeat the same procedure above. Then, 400µl of RNA wash buffer was mixed into columns and followed the protocol mentioned above so that the sample was mixed thoroughly. The column was transferred to micro-centrifuge, and then 50µl of DNase/RNase-Free Water was added. The column was left for five minutes and then centrifuged for 30 seconds at 16000 xg to separate RNA concentration from the column. Finally, the obtained RNA was stored at -80°C.

The isolated RNA of critical-sized bone defect samples was quantified using a nanodrop machine (BioDrop-µLite+spectrophotometer (BioChrom)). The nanodrop plate (Thermo Scientific) was wiped with lens tissue damped with distilled water, followed by 70% ethanol to remove contaminants. 2µl of the purified RNA of each sample was pipetted onto the nanodrop plate. The concentrations (µg/ml) and purities (A260/A280 and A260/A230) were obtained. The quantified

RNA samples were diluted in nuclease-free water (NFW) using the formula $V_1 \times C_1 = V_2 \times C_2$ so that all the samples have a final concentration of 50ng/µl or 50 µg/ml.

Microarray Analysis of miRNA

Total miRNA extraction was conducted following the instructions provided by the Zymo Research kit. The miRNA library chip was procured from Genetic Science Human V3 miRNA assay CSO. With NanoString nCounter Human v3 miRNA Expression Assay (NS_H_miR_v3b) kit (CSO-MIR3-12), 3µl miRNA was ligated to mir-Tag with ligation buffer and Ligase supplied with the kit. After being diluted with 15 µl of nuclease-free water, the ligated product was denatured for five minutes at 85ºC. 5 µl of the product was hybridized overnight at 65°C with reporter and capture probes. The protocol was followed in accordance with the user manual (MAN-C0009-07, Counter miRNA Expression Assay User Manual). ADMSCs-EVs sample was assessed using the nCounter Analysis System (from NanoString Technologies) and the nCounter Human v3 miRNA Expression Assay (NS_H_miR_v3b) panel, which includes 799 unique miRNA barcodes for endogenous miRNA. The housekeeping genes incorporated in the panel include beta-actin (ACTB), beta-2-microglobulin (B2M), glyceraldehyde 3-phosphate dehydrogenase (GAPDH), ribosomal protein L19 (RPL19), and ribosomal protein lateral stalk subunit P0 (RPLP0).[17]

In Vivo Animal Experiment

In calculating the sample size for this study, Federer's formula was used: $(t - 1)(n - 1) \geq 15$, where t is the number of treatment groups and n is the number of samples. With t=3, n must be greater than or equal to 8.5.[11] A total of 20 SD rats were allocated randomly into three groups: Group 1 (Four SD rats as healthy/positive control), group 2 (eight SD rats as NaCl/negative control), and Group 3 (8 SD rats as ADMSCs-EVs/intervention group). A 5 mm critical-sized femoral bone defect was created in groups 2 and 3. Furthermore, 1.4 mm intramedullary Kirschner wires were internally fixated to stabilise the bone gap. Group 2 underwent implantation of 0.4cc of NaCl 0.9% (Indonesia-GKL2012431149A1) by directly pouring on the area of the bone defect. Group 3 was implanted with 0.4cc of ADMSCs-EVs by directly pouring on the area of the bone defect.

Animals were kept in an isolated cage system. They were fed and given antibiotics to prevent infection at the Animal Research Facilities, IMERI. Rats were terminated on two separate timelines, on the 14th and 28th days of surgery. The bone defect samples were divided into two longitudinal sections carrying the highest proportion of bone defect area. One of the two longitudinal sections was preserved in a 10% formalin solution (India – 531140) for histological processing and immunohistochemistry, while the other was preserved in a DNA/RNA Shield™ (1X) (R1100-250 Zymo Research, USA) for molecular processing to assess the expression of collagen area %, chordin, and Wnt 3A expressions. Moreover, BMP2 ELISA was also performed to determine the BMP2 protein concentration.

Histology Analysis

Critical-sized bone defect samples were fixed in 10% formol saline and then dehydrated using gradually increasing ethanol concentrations (Smartlab A 1035, Indonesia). Samples were cleared in xylol (Smartlab A 1079, Indonesia) and embedded in paraffin before hematoxylin and eosin (HE) staining to observe morphology. HE staining was carried out using deparaffinization of histological slides with xylol and rehydration by decreasing grades of alcohol (100%, 96%, 80%, and 70%). The preparations were then incubated in hematoxylin solution (Indonesia – 10201026900), washed with running water for a short time, and continued with eosin incubation (AKD 10201320404, Indonesia). The preparation was covered with Entellan (Merck HX03691561, USA) and a cover slip.

Mason Trichrome (MT) staining was carried out by deparaffinizing histological slides with xylol and rehydration by soaking in decreasing graded alcohol (100%, 96%, 80%, and 70%). The preparation was then put into Bouin's fixative solution and soaked in Weigert hematoxylin solution and Biebrich scarlet acid fuchsin solution. The preparation was then immersed in phosphomolybdic acid and incubated in aniline blue. The results from the microphoto with Optilab were then analyzed with Image J® software to quantify the percentage collagen area on MT staining.

qRT-PCR of chordin, Wnt3A and Spp1

RNA Isolation Kit (Quick RNA Miniprep plus, Zymo®)wasusedforRNAextractionfromhomogenized samples according to the manufacturer's instructions, as mentioned above in the total RNA extraction section. cDNA synthesis was done using the Master Mix (FSQ 301- Toyobo, Japan) with gDNA remover (Toyobo) on a thermal cycler (Applied Biosystem Veriti 96well). The incubation time for cDNA synthesis was 37°C for 15 minutes, 50°C for 5 minutes, then 98°C for 5 minutes in Veriti™ 96-Well Thermal Cycler.

qRT-PCR was performed using SensiFAST™ SYBR Lo-ROX Kit (Bioline) with 7500 Fast Real-Time PCR System (Applied Biosystems). The qRT-PCR was done in triplicate for each sample with 3.2 ng of cDNA per reaction. The total number of cycles in qRT-PCR was 40 cycles. The conditions for qRT-PCR were polymerase activation at 95°C for 2 minutes, denaturation at 95°C for 5 seconds, annealing at 55.5°C (for chordin and Spp1) and 58°C (for Wnt3A), and extension in 72°C for 25 seconds. Ct values were normalized to the housekeeping gene GAPDH. Sequences for Spp1 and chordin were designed using NCBI and IDT PrimerQuest software. Wnt3A sequence was obtained from Yan et al.[18] The GAPDH gene was obtained from Puji et al.[19] Primer sequences used are listed in Table 1.

Tabel 1. Primer mRNA

Genes	Primer Sequence
Spp1	F:TCCATGTGGACGCTCTTTCA
	R: AGCAGCAACGCTAGAAGACA
Chordin	F:GGTCTATGCCTTGGACGAGA
	R: TGGTTTGATGTTCTTGCAGCTG
Wnt3A	F:TTCTGTGAGCCCAACCC
	R: CAGCACCAGTGGAAGACG
GAPDH	F:CCCTTCATTGACCTCAACTACA
	R: ATGACAAGCTTCCCGTTCTC

Table 2. Positive miRNA Count

miR	Library Code	Expression Of miR From EVs ADMSC	Expression Ratio Of miR Against The Housekeeping Gene (ACTB)
Bone Regeneration-related miRNAs with no specific signalling pathway			
hsa-miR-129-5p	MIMAT0000242	10	0.5
hsa-miR-140-3p	MIMAT0004597	12	0.6
hsa-miR-142-3p	MIMAT0000434	8	0.4
hsa-miR-142-5p	MIMAT0000433	6	0.3
hsa-miR-190a-5p	MIMAT0000458	3	0.15
hsa-miR-199b-5p	MIMAT0000263	12	0.6
hsa-miR-217	MIMAT0000274	26	1.3
hsa-miR-335-5p	MIMAT0000765	7	0.35
hsa-miR-140-5p	MIMAT0000431	8	0.4
Specific BMP2 Signaling Pathway Regulators			
hsa-miR-93-5p	MIMAT0000093	22	1.1
hsa-miR-375	MIMAT0000728	6	0.3
Specific Wnt Signaling Pathway Regulators			
hsa-miR-433-3p	MIMAT0001627	7	0.35
hsa-miR-542-3p	MIMAT0003389	13	0.65
hsa-miR-328-3p	MIMAT0000752	6	0.3
ACTB	NM_001101.2	20	1

BMP2 Enzyme-linked Immunosorbent Assay Analysis

The preparation of samples includes thawing the homogenate samples stored at -80°C. The concentration of BMP2 protein was quantified using an enzyme-linked immunosorbent assay (ELISA) (bio-tchne®, R&D Systems, USA- DBP200) according to the manufacturer›s instructions. Absorbance was measured at 450 nm using an ELISA reader (Thermoscientific).

Statistical Analysis

The normality test of Saphiro-Willk is done for each group before the analysis. Statistical analysis was performed with the One-Way ANOVA test using GraphPad Prism 10.1.0 when data is normally distributed.

Results

The EVs were successfully isolated from ADMSCs using the ultracentrifugation technique

following the copyright protocol established in SCTE IMERI.[16] The characterization of ADMSCs-EVs (exosomes) was described in Supplementary File 1*.

miRNA Microarray Analysis

From the results of the microarray analysis, we focus on 14 miRNAs that have a role in bone regeneration signalling pathways, specifically BMP2 and Wnt. miRNA count and ratio between miRNA and housekeeping genes are listed in Table 2.

In Table 2, the housekeeping gene ACTB has an expression ratio of 1. miR-217 and miR-93-5p have an expression ratio of more than 1, showing that they are upregulated (Figure 1). The remaining miR have an expression ratio of less than 1, showing that they are downregulated. From microarray analysis, miR-217 has most of the expression of 26, showing that this miR is abundant in ADMSCs-EVs. miR-93-5p is also present in

significant amounts. miR-190a-5p has the slightest expression of 3 in ADMSCs-EVs.

Figure 1 shows the ratio of miRNA expression downregulated from ADMSCs-EVs found through microarray analysis. We found that 11 miRNAs were significantly downregulated, showing that they had a minimal effect on bone regeneration. miR-433-3p, miR-542-3p and miR-328-3p are found to work synergistically with Wnt signalling, showing that they have a role in bone regeneration.

Two upregulated miRNAs have been identified, miR-93-5p and miR-217, that may function as regulators of bone regeneration (Figure 1). miR-93-5p is found to have a negative role in the BMP2 signalling pathway. Stitched microphotographs (Figure 2) for HE staining showed that in the EVs-treated group, there was an initial bridge of soft callus on day 14 and more soft callus formation on day 28. However, in NaCl treated group, there is no union of bone fragments at all at day 14 and day 28.
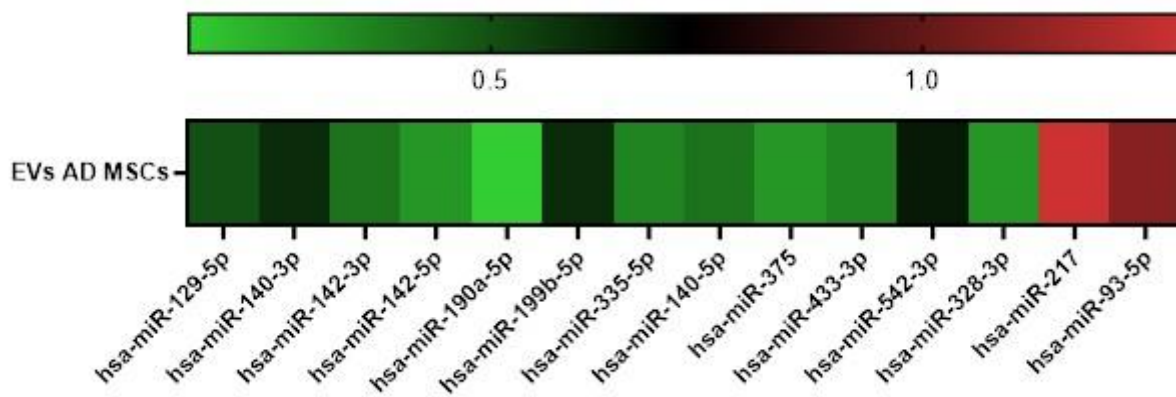

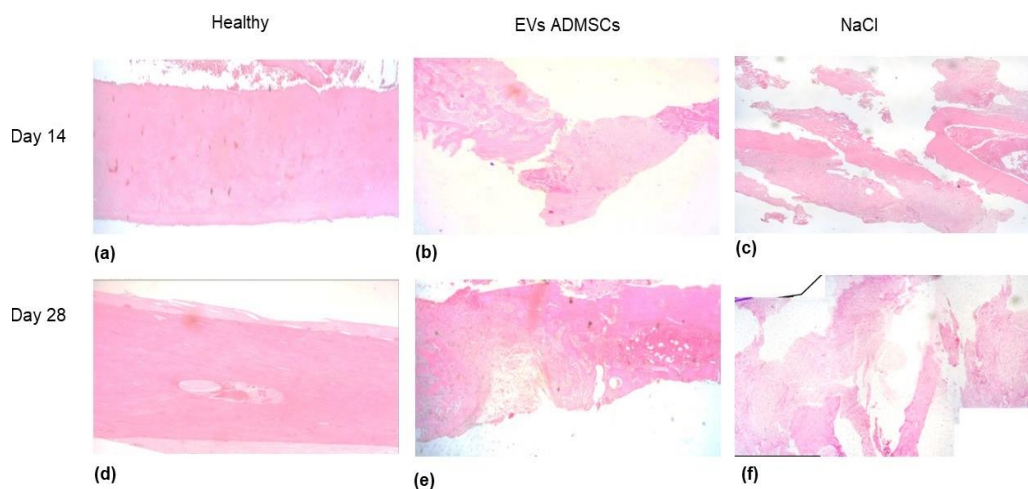**Figure 1. Heatmap of ADMSCs EVs miRNA Expression**

Figure 2. HE Staining at Days 14 and 28 (a) Healthy Sample at Day 14 (b) ADMSCs-EVs Treated Sample at Day 14 (c) NaCl Treated Sample at Day 14 (d) Healthy Sample at Day 28 (e) ADMSCs-EVs Treated Sample at Day 28 (f) NaCl Treated Sample at Day 28
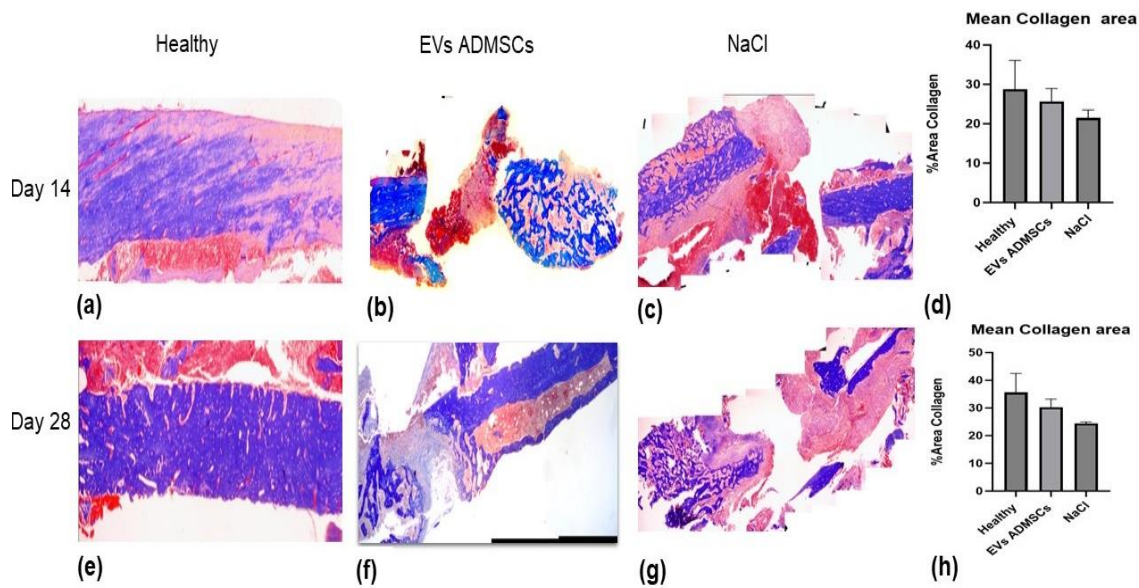
Figure 3. Representative Pictures of Masson Trichrome Staining on Days 14 and 28 and Mean Collagen Area from MT Stained Slides (a) Healthy Sample at Day 14 (b) ADMSCs-Evs Treated Sample at Day 14 (c) NaCl Treated Sample at Day 14 (d) Mean Collagen Area at Day 14 € Healthy Sample at Day 28 (f) ADMSCs-EVs Treated Sample at Day 28 (g) NaClTreated Sample at Day 28 (h) Mean Collagen Area at Day 28

According to stitched microphotographs (Figure 3) for MT staining, initial soft callus formed the critical size bone defect areas in the EVs-treated group. However, the bone fragments were not aligned on day 14. The EVs-treated group showed a soft callus bridge on day 28 with alignment of the bone fragments. The group that underwent NaCl treatment on day 14 shows that the alignment of bone fragments is lost with the absence of soft callus formation. On day 28, the alignment of bone fragments appears with very little soft callus bridge.

In the measurements with ImageJ in Figure 3 (d, h), it was found that the mean percentage of collagen area with standard error of the mean in the ADMSCs-EVs group was 25.65% ±1.65% and 30.32% ±1.43% at day 14 and day 28, respectively. The mean percentage of collagen area in the NaCl group was 21.53% ± 0.99% at day 14 and 24.97% ±0.63% at day 28. The one-way ANOVA test revealed no statistically significant differences in collagen area results between groups at day 14 (p>0.05). However, there was a significant difference between groups on day 28 (p=0.01).

BMP2 ELISA Analysis and qRT PCR of Chordin

The standard curve of BMP2 ELISA is linear, showing that standards are good. The value of absorbance reading is y= 0.00020618x + 0.0310584 with R^2 = 0.998. The value of R^2 is showing that the standard curve is linear (Figure 3). The mean BMP2 level at day 14 in the ADMSCs-EVs treated group was 95.20 pg/ml (Figure 4a), while in the negative control (NaCl group), it was 24.44 pg/ml (Figure 4b). There was no significant difference between groups at day 14 (P>0.05). At day 28, the ADMSCs-EVs and NaCl groups demonstrated nearly identical mean BMP2 protein levels of 86.66 pg/ml and 85.69 pg/ml, respectively, with no significant difference (p>0.05).

The mean normalized chordin gene expression at day 14 (Figure 4c) was 0.24 in the ADMSCs-EVs treated group and 0 in the NaCl group. At day 28 (Figure 4d), the mean normalized chordin gene expression was 5.73 in the ADMSCs-EVs treated group and 0.01 in the NaCl group.

Wnt 3A and Spp1 Gene Expression

The mean normalized Wnt3A gene expression at day 14 (Figure 5a) was 2.56 in the ADMSCs-EVs treated group and 2.43 in the NaCl group. At day 28 (Figure 5b), the mean normalized Wnt3A gene expression was 0.04 in the ADMSCs-EVs treated group and 0.03 in the NaCl group.
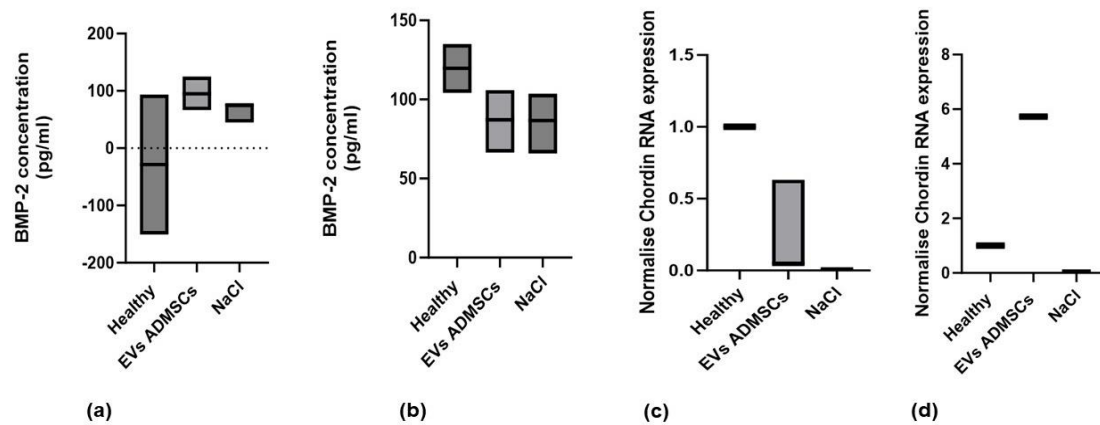
Figure 4. BMP2 Protein Concentration and Chordin Gene Expression (Antagonist of BMP2) (a) BMP2 Protein Concentration at 14 Day (b) BMP2 Protein Concentration at 28 Day (c) Chordin Gene Expression at 14 Day (d) Chordin Gene Expression at 28 Day
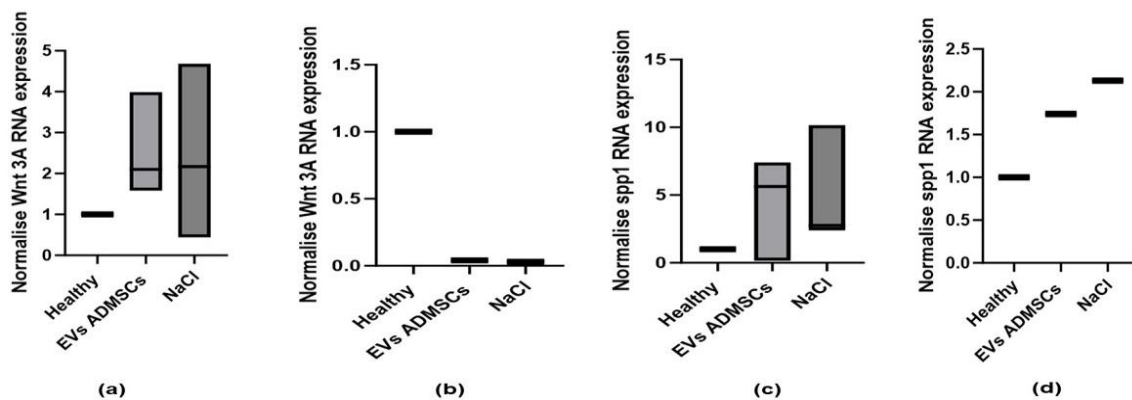

Figure 5. Wnt 3A and Spp1 Gene Expression (Downstream of BMP2 and Wnt Signalling) (a) Wnt 3A Gene Expression at 14 Day (b) Wnt 3A Gene Expression At 28 Day (c) Spp1 Gene Expression at 14 Day (d) Spp1 Gene Expression at 28 Day

In Figure 5c, the mean normalized Spp1 gene expression at day 14 was 4.40 in the group treated with ADMSCs-EVs. In contrast, the NaCl-treated group exhibited a slightly higher mean expression level of 5.10. On day 28 (Figure 5d), a notable decrease in the mean normalized Spp1 gene expression was observed in the ADMSCs-EVs treated group, with a value of 1.74. Similarly, the NaCl-treated group also showed a decrease in mean expression, with a value of 2.13.

Discussion

This study identified 14 miRNAs from ADMSCs-EVs involved in critical-sized bone defect regeneration signalling pathways, emphasising BMP2 and Wnt signalling. Among 14 miRNAs, two upregulated miRNAs (miR-93-5p and miR-217), specifically miRNA-93-5p, inhibit the BMP2 signalling pathways.[20] While other 12 miRNAs were downregulated (miR-129-5p, miR-140-3p, miR142-3p, miR-142-5p, miR-190a-5p, miR-199b-5p, miR-335-5p, miR-140-5p, miR-375, miR-433-3p, miR-542-3p and miR-328-3p). Downregulated miRNAs, miR-433-3p, miR-542-3p, and miR-328-3p, enhanced the Wnt signalling pathway.[20,21] Soft callus formation appeared at critical size bone defect area with a higher proportion in the ADMSCs-EVs group at day 28. Results of this study showed that EVs are superior in inducing soft callus formation than the NaCl group (negative control). The peak

period of chondrogenesis was seen at 14 days in the study by Gerstenfeld et al.[22] Our result showed histology of soft callus mainly composed of fibrous connective tissue with no signs of chondrogenesis.

The mean collagen area fraction in the ADMSCs-EVs treated group is higher than the NaCl-treated group at day 14 and persistently higher at day 28 in the ADMSCs-EVs treated group. Significant differences in collagen area fraction at day 28 strengthen the proof of increased soft callus formation in the ADMSCs-EVs treated group. Previous studies showed that the EVs BM MSCs treated group revealed an absence of alignment of fracture gaps on day 14 and a callus on day 21. Further, a larger callus formation, which covered fracture gaps on day 28, was observed.[23] The histology findings comparable with our study are the difference in the source of EVs MSCs with partial coverage of the bone defect gaps. It showed that EVs carried inductive signals for osteoprogenitor cells in the bone marrow and the periosteum at sites of the critical-size bone defect. These signals target the internal machinery of the cells to start osteogenic differentiation at the bone defect gaps. However, EVs can not regenerate bone defect gaps as a single agent. Proper bone defect alignment and retention material, provided by scaffold or extracellular matrix and additional growth factors or combined cytokines, proved to be superior to ADMSCs-EVs alone. A study by an orthopedic surgeon from FMUI-Cipto Mangunkusumo Hospital showed that ADMSCs-EVs combined with hydroxyapatite (HA), platelet-rich fibrin (PRF), and bone graft showed improved critical bone defect regeneration in the rat model.[24]

The inhibition of the BMP2 signalling pathway by ADMSCs- EVs, along with the upregulation of miR-93-5p observed in our study, is confirmed by the BMP2 ELISA and qRT-PCR results for chordin. The BMP2 level in the EVs ADMSCs treated group on day 28 was relatively lower than that of the negative control group (NaCl). This is further confirmed by qRTPCR results, revealing that chordin, the antagonist of BMP2, is highest in the ADMSCs- EVs group. In line with the downregulation of miR-433-3p, miR-542-3p, and miR-328-3p in EVs AD MSCs, the subsequent promotion of the Wnt signalling pathway is confirmed by the qRTPCR results of Wnt 3A. Wnt3A expression is high in the ADMSCs-EVs group on day 14, returning to the basal expression on day 28. The wnt3A expression

of the EVs AD MSCs treated group is similar to that of the negative control group on days 14 and 28. Spp1, downstream of the BMP2 and Wnt signalling pathways[25,] showed that Spp1 expression remains high on days 14 and 28. Changes in BMP2, Wnt3A, and Spp1 expression indicated that the specific miRNA inside ADMSCs-EVs alters the signalling pathway in the bone defect microenvironment. Overall signalling appears linear with the delayed critical size bone defect regeneration of the ADMSCs-EVs treated group. The inhibition of BMP2 and transient increase of the Wnt signalling pathway could not provide adequate sustained signalling for bone regeneration.

The limitations of this study are the lack of documentation of post-surgery clinical outcomes in SD rats, physiological parameters, e.g. gait analysis for assessing functional recovery, and limited molecular analysis data. Further investigation is needed to determine the optimal dose of miRNA within EVs for regulating BMP2 and Wnt signalling, a crucial step in advancing critical bone defect regeneration. Additionally, exploring the retention time of EVs within critical bone defects post-surgery would provide valuable insights into their therapeutic efficacy and bioavailability for sustained impact on bone regeneration.

Conclusion

Specific miRNA inside ADMSCs-EVs regulates BMP-2 and Wnt signalling to enhance soft callus formation in critical-size bone defects.

Acknowledgment

*Please contact the corresponding author for data availability

References

1. Keating JF, Simpson AHRW, Robinson CM. The management of fractures with bone loss. J Bone Joint Surg Am. 2005;87:142–50. doi: 10.1302/0301-620x.87b2.15874

2. Huang EE, Zhang N, Shen H, Li X, Maruyama M, Utsunomiya T, et al. Novel techniques and future perspective for investigating critical-size bone defects. Bioengineering. 2022;9:171. doi: 10.3390/bioengineering9040171

3. Norris BL, Vanderkarr M, Sparks C, Chitnis AS, Ray B, Holy CE. Treatments, cost and healthcare utilization of patients with segmental bone defects. Injury. 2021;52:2935–40. doi: 10.1016/j.injury.2021.01.016

4. Amini AR, Laurencin CT, Nukavarapu SP. Bone tissue engineering: recent advances and challenges. Crit Rev Biomed Eng. 2012;40:363-408. doi: 10.1615/critrevbiomedeng.v40.i5.10

5. Ferdiansyah, Rushadi D, Rantam FA, Aulani'am. Regeneration of massive bone defect with bovine hydroxyapatite as scaffold of mesenchymal stem cells. JBP. 2011;13:179-95.

6. Dilogo IH, Phedy P, Kholinne E, Jusuf AA, Yulisa ND. Role of allogeneic mesenchymal stem cells in the reconstruction of bone defect in rabbits. MJI. 2014;23:9-14. doi: 10.13181/mji.v23i1.683

7. Dilogo IH, Pramantha B, Kodrat E, Anggraini R. Comparison of regeneration between human bone marrow and adipose mesenchymal stem cells on the treatment of critical size bone defect in *Sprague dawley* rats. ARRB. 2017;19:1-9. doi: 10.9734/ARRB/2017/37318

8. Mauffrey C, Barlow BT, Smith W. Management of segmental bone defects. JAAOS. 2015;143–53. doi: 10.5435/JAAOS-D-14-00018

9. Oryan A, Alidadi S, Moshiri A, Maffulli N. Bone regenerative medicine: classic options, novel strategies, and future directions. J Orthop Surg Res. 2014;9:18. doi: 10.1186/1749-799X-9-18

10. Oryan A, Kamali A, Moshirib A, Eslaminejad MB. Role of mesenchymal stem cells in bone regenerative medicine: what is the evidence? Cells Tissues Organs. 2017;204:59–83. doi: 10.1159/000469704

11. Zomorodian E, Baghaban Eslaminejad M. Mesenchymal stem cells as a potent cell source for bone regeneration. Stem Cells Int. 2012;2012:980353. doi: 10.1155/2012/980353

12. Pawitan JA, Liem IK, Suryani D, Bustami A, Purwoko RY. Simple lipoaspirate washing using a coffee filter. Asian Biomed. 2013;7:333-8. doi: 10.5372/1905-7415.0703.184

13. Schubert T, Lafont S, Beaurin G, Grisay G, Behets C, Gianello P, et al. Critical size bone defect reconstruction by an autologous 3D osteogenic-like tissue derived from differentiated adipose MSCs. Biomaterials. 2013;34:4428-38. doi: 10.1016/j.biomaterials.2013.02.053

14. Fiolin J, Dilogo IH, Antarianto RD, Pontoh LA. Isolation and characterization of adipose-derived mesenchymal stem cell exosomes: an in-vitro study. Jurnal Kedokteran dan Kesehatan. 2022;16:108-112. doi: 10.33533/jpm.v16i2.4867

15. Tan SHS, Wong JRY, Sim SJY, Tjio CKE, Wong KL, Chew JRJ, et al. Mesenchymal stem cell exosomes in bone regenerative strategies-a systematic review of preclinical studies. Mater Today Bio. 2020;7:100067. doi: 10.1016/j.mtbio.2020.100067

16. Antarianto RD, Pragiwaksana A, Humairoh N. Surat pencatatan ciptaan. EC002022103579. Jakarta: Direktorat Jenderal Kekayaaan Intelektual Kementerian Hukum dan HAM RI; 2022.

17. Shankar M, Shetty A, Tennankore K. Urinary exosomal miRNA signature of IgA nephropathy: a case–control study. Sc Rep. 2023;13:21400. doi: 10.1038/s41598-023-47751-z

18. Yan YB, Li JM, Xiao E, An JG, Gan YH, Zhang Y. A pilot trial on the molecular pathophysiology of traumatic temporomandibular joint bony ankylosis in a sheep model. Part I: expression of Wnt signaling. J Craniomaxillofac Surg. 2014;42:e15-2. doi: 10.1016/j.jcms.2013.04.009

19. Livak KJ, Schmittgen TD. Analysis of relative gene expression data using real-time quantitative PCR and the 2-ΔΔCT method. Methods. 2001;25:402–8. doi: 10.1006/meth.2001.1262

20. Iaquinta MR, Lanzillotti C, Mazziotta C, Bononi I, Frontini F, Mazzoni E, et al. The role of microRNAs in the osteogenic and chondrogenic differentiation of mesenchymal stem cells and bone pathologies. Theranostics. 2021;11:6573-91. doi: 10.7150/thno.55664

21. Guan S, Zhang Z, Wu J. Non-coding RNA delivery for bone tissue engineering: progress, challenges, and potential solutions. iScience. 2022;25:104807. doi: 10.1016/j.isci.2022.104807

22. Gerstenfeld LC, Alkhiary YM, Krall EA, Nicholls FH, Stapleton SN, Fitch JL, et al. Three-dimensional reconstruction of fracture callus morphogenesis. JHC. 2006;54:1215-28. doi: 10.1369/jhc.6A6959.2006

23. Xu T, Luo Y, Wang J, Zhang N, Gu C, Li L, et al. Exosomal miRNA-128-3p from mesenchymal stem cells of aged rats regulates osteogenesis and bone fracture healing by targeting Smad5. J Nanobiotechnology. 2020;18:1-8. doi: 10.1186/s12951-020-00601-w

24. Hilmy F, Dilogo IH, Reksodiputro MH, Antarianto RD, Al Mashur MI, Adhimulia KJ. Evaluation of adipose-derived stem cells (ASCs) exosome implantation and plateletrich fibrin (prf) on critical long bone defects in sprague-dawley rats. Eur J Orthop Surg Traumatol. 2024;34:2805-10. doi: 10.1007/s00590-024-03964-0

25. Thomas S, Jaganathan BG. Signaling network regulating osteogenesis in mesenchymal stem cells. J Cell Commun Signal. 2022;16:47-61. doi: 10.1007/s12079-021-00635-1